

## Oxygen Reduction at Thin Copper Manganite Spinel Films. Kinetic Parameters, Temperature and Apparent Enthalpies of Activation

A.F. Restovic

Departamento de Química, Facultad de Ciencias Básicas, Universidad de Antofagasta,  
Casilla 170, Antofagasta, Chile

J.L. Gautier\*

Departamento de Química, Facultad de Ciencia, Universidad de Santiago,  
Casilla 5659, Santiago 2, Chile

Received: May 31, 1994; October 5, 1994

Estudou-se a reação de redução de oxigênio (ORR) sobre eletrodos recobertos por filmes finos de  $\text{Cu}_{1+x}\text{Mn}_{2-x}\text{O}_4$  ( $0.4 \geq x \geq 0$ ) tipo spinel, em soluções aquosas de KOH, a temperaturas de 298 a 338 K e pHs de 12 a 14. Em todas as temperaturas, foram observadas duas diferentes regiões lineares E-log *i*. Foram obtidos coeficientes angulares de Tafel de  $\approx 60 \text{ mV dec}^{-1}$ , para baixos potenciais, e de  $\approx 120 \text{ mV dec}^{-1}$ , para altos potenciais aplicados. Em todos os casos, a ordem de reação com relação ao oxigênio é 1. A ordem de reação com relação aos íons  $\text{OH}^-$  mudava para valores fracionários em função do potencial. A partir do comportamento das entalpias aparentes de ativação ( $\Delta H^*$ ), que varia com o pH e o potencial aplicado, foi possível propor o mecanismo provável da ORR. O valor de  $\Delta H^*_{E=0}$  da reação depende também da estequiometria do óxido (*x*). A ORR nestes materiais é influenciada pela concentração e pela natureza química dos íons do óxido superficial.

Oxygen reduction reaction (ORR) at  $\text{Cu}_{1+x}\text{Mn}_{2-x}\text{O}_4$  ( $0.4 \geq x \geq 0$ ) thin film spinel electrodes in aqueous KOH solutions was examined at temperatures from 298 to 338 K, and at pHs from 12 to 14. At all temperatures two different linear E-log *i* regions were observed. The Tafel slopes were found to be  $\approx 60 \text{ mV dec}^{-1}$  at a low potential and  $\approx 120 \text{ mV dec}^{-1}$  at a high applied potential. For all cases studied, the reaction order with respect to oxygen is 1. The reaction order with respect to  $\text{OH}^-$  ions changed to a fractional order as a function of the potential. From the behavior of apparent activation enthalpies ( $\Delta H^*$ ), which change with pH and applied potential, it was possible to propose a probable ORR mechanism.  $\Delta H^*_{E=0}$  of the reaction also depends on oxide stoichiometry (*x*). The ORR of these materials is affected by the concentration and chemical nature of the surface oxide ions.

**Keywords:** copper manganites, mixed oxides, electrocatalysis, enthalpies of activation, oxygen reduction

### Introduction

Among the inorganic electrocatalysts studied for the oxygen reduction reaction (ORR), mixed oxides of the transition elements with spinel structure have been proved to be efficient electrodes<sup>1,2</sup>.

Studies of ORR in alkaline solutions on rotating disk electrodes with a disk of  $\text{Cu}_{(1+x)}\text{Mn}_{(2-x)}\text{O}_4$  ( $0.4 \geq x \geq 0$ ) prepared in a pellet or thin film form have shown that the electrocatalytic activity of the oxides increases in both preparations when the copper concentration in the solid increases<sup>3-5</sup>. Typical current densities have been found to

be  $3 - 9 \cdot 10^{-7} \text{ A/cm}^2$  (thin films) and  $3 - 15 \cdot 10^{-9} \text{ A/cm}^2$  (pellet) for  $x = 0$  and  $x = 0.4$ , respectively. These values have been explained by considering the different roughness factors associated with the method of preparation and surface site concentration<sup>5</sup>. With both electrode preparations, the ORR is characterized by two E-*j* regions as a function of the applied potential. At a low potential (l.p.), the Tafel slope is  $-RT/F$ , while at a high potential (h.p.) it is  $-2RT/F$ . The reaction order with respect to molecular oxygen and hydroxyl ions in the l.p. region were found to be  $p_{\text{O}_2} = 1$  and  $p_{\text{OH}^-} = -1$ , respectively, according to a proposed mechanism<sup>6,7</sup>. At l.p., the superoxide ion protonation seems to be

the rds, while at h.p. the first electron transfer will be the rds. Similar E-j behavior has been found with metal-cobaltites<sup>8</sup>. Two Tafel slopes have also been observed in studying the OER on similar thin film copper manganese oxide electrocatalysts<sup>9</sup>.

The electrochemical free energy of activation for ORR depends on the chemical and electrical contributions  $\Delta\tilde{G}^* = \Delta G^* + \alpha FE$ . The activation barrier value is decreased by the adsorption of oxygen-intermediates in the rds and the Fermi level of the electrons at the oxide surface which is affected as a shift in  $\Delta G^*$  through  $FE\alpha$ . Different adsorption conditions can change the Tafel slopes. The transfer coefficient is assumed to be temperature dependent and is associated with the enthalpic and entropic component<sup>10</sup>,  $\alpha = \alpha_H + \alpha_S T$ . According to the ORR mechanism in copper-manganites (in the pellet form) already proposed<sup>6</sup>, the electrocatalytic current can be written as  $j = 2F k_{app} pO_2 (1/C_{OH^-}) \exp(\alpha_S FE/R) \exp(-\alpha_H FE/R) 1/T = A \exp(-\alpha_H FE/R)$ , where  $k_{app} = \kappa(kT/h) \exp(-\Delta H^*/RT) \exp(\Delta S^*/R) \exp(-\alpha F \Delta \phi_{ref}/RT)$ ,  $\kappa$  is the Henry constant, and  $\Delta H^* = -2.303 (\partial \log j / \partial T^{-1})_{C_{OH^-}, E}$ , is the apparent enthalpy of activation. The enthalpy activation values obtained at l.p. and h.p. have been used to confirm the reaction mechanism by which the change in the adsorption conditions with O-intermediates at a critical coverage ( $\theta$ ) occur at  $E = cst$ <sup>11</sup>. On the other hand, it is interesting to correlate the Tafel slopes of ORR with temperature because the enthalpic and entropic components can be determined by using an adequate reaction mechanism. The electrocatalytic activity of  $Cu_{1+x}Mn_{2-x}O_4$  thin films increased with copper stoichiometry, as had been determined at room temperature<sup>5,12</sup>. The ORR Tafel slopes at l.p. and h.p. decreased with x: - 69, - 130 (x = 0); - 67, - 128 (x = 0.1); - 65, 126 (x = 0.2); - 60, - 116 (x = 0.3); - 60, 112 ± 2 mV/dec (x = 0.4), respectively.

In this work, the kinetic parameters of the ORR in 1 M KOH as a function of temperature at  $Cu_{(1+x)}Mn_{(2-x)}O_4$  electrodes with  $0.4 \geq x \geq 0$  were studied. The ORR thermodynamic parameters have been largely investigated in the case of noble metals<sup>11,13</sup>, in contrast to mixed oxides. To our knowledge, this is the first time that spinel manganite electrodes have been studied in this way and the results offer the possibility of correlating them with oxide cationic structures. It has been suggested that electrocatalysis occurs through oxygen adsorption on active oxide sites formed by  $Mn^{4+}$  ions associated with  $Mn^{3+}$  ions in octahedral sites of the spinel cell unit<sup>12</sup>.

## Experimental

### Chemical synthesis

The polycrystalline compounds  $Cu_{1+x}Mn_{2-x}O_4$  ( $0.4 \geq x \geq 0$ ) were synthesized by the spray pyrolysis technique. This technique consists of spraying, at room temperature, an aqueous solution of metallic salts, prepared with stoichiometric amounts of  $Cu(NO_3)_2 \cdot 3H_2O$  p.a. (Merck,

ref. 2752) and  $Mn(NO_3)_2 \cdot 4H_2O$  p.a. (Riedel de Haen, ref. 31423) dissolved in aqueous solution, slightly acidic, and contains n-butanol. It also involves the use of a convenient gas vector, on an appropriate substrate, which is simultaneously heated at selected temperatures. The experimental setup used in this work was the same as previously reported<sup>14</sup>. The whole unit consisted of a vertical furnace, containing the substrate (the temperature was maintained constant within 10 °C by an electronically controlled unit and placed in a glass bell-jar), the spray nozzle (inserted through a hole on one side of the bell-jar, which had another hole for the vapors to escape), and the spray solution container, and was enclosed in a chamber with an exhaust fan to remove the gases and vapors produced during spraying.

The oxides were prepared at 530 °C using the same nitrate solutions employed for ceramic preparation in pellet form<sup>6,7</sup>, which were sprayed on nickel foils (Aldrich, ref. 26825), then submitted to a thermal treatment taking into account the published phase diagrams<sup>15</sup>. The preparation details, particularly the effect of deposited oxide weight and the substrate nature of  $Cu_{1.4}Mn_{1.6}O_4$  morphology and electrical properties have been described elsewhere<sup>9</sup>.

### Characterization

All samples were stored in an argon-filled desiccator. They were characterized by X-ray powder diffraction recorded with a Philips diffractometer 1050-80. Copper and manganese contents were checked with a Perkin Elmer 1100 Atomic Absorption Spectrophotometer. Electrical conductivity measurements were made in a vacuum ( $10^{-2}$  Torr), as a function of temperature, using a Jandel bridge and a powder cell<sup>16</sup>.

The electrochemical measurements were determined in the stationary state. The experiments were performed at temperatures from 298 K to 338 K in 1MKOH solutions, using a potentiostat PINE RD3 and an XY Graphtec 4500 recorder. The reference electrode was Hg/HgO/1MKOH (0.098V vs. SHE). The potentials measured were related to this electrode under isothermal conditions. A conventional three electrode cell was used. The oxide samples mentioned above were introduced on the terminal of the Tacussel EAD 4500 rotating disk electrode. The angular frequency of the rotating electrode was  $425 \text{ s}^{-1}$ , controlled with an optical tachometer. Before use, the electrode surface was polished with a BSC3 Tacussel polishing ribbon. The electrolytic solution was prepared from analytical grade KOH pellets and doubly distilled water. The solutions were electrolyzed using Pt electrodes under an argon atmosphere immediately before use. IR-correction and mass transfer effects were considered.

## Results

The oxides prepared by the technique described above, crystallizing in spinel phase,  $AB_2O_4$ , space group  $Fd3m$ ,

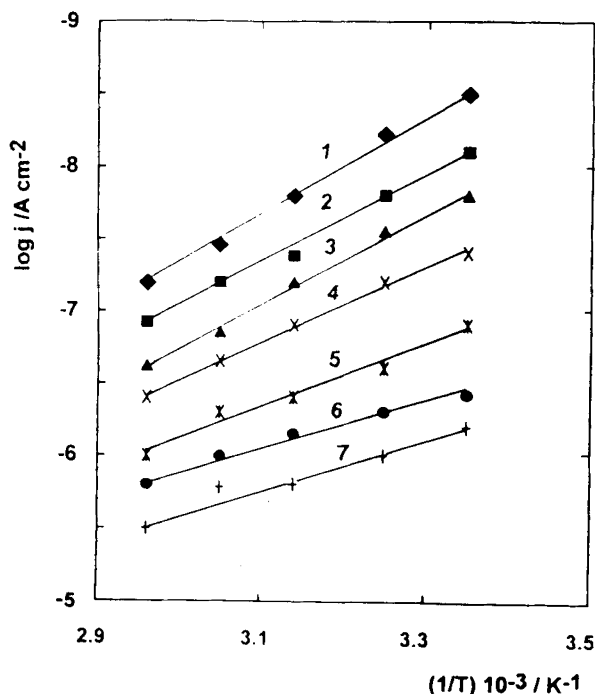
and no parasitic phases or impurities were detected by chemical analysis. The unit cell "a" decreases as a function of copper concentration,  $a = 0.837; 0.834; 0.833; 0.830; 0.829$  nm for  $x = 0; 0.1; 0.2; 0.3$  and  $0.4$ , respectively. The oxide ionic distribution for  $0.3 \geq x \geq 0$  obeys the following general formulae which consider the presence of copper ions,  $\text{Cu}^+$  and  $\text{Cu}^{2+}$ , placed in tetrahedral and octahedral oxygen coordination, respectively,  $\text{Cu}_a^+ \text{Mn}^{2+}_{(1-a)} [\text{Cu}^{2+}_{(1+x-a)} \text{Mn}^{3+}_{(a-2x)} \text{Mn}^{4+}_{(1+x)}] \text{O}^{2-}_4$ . In the case of  $x = 0.4$ , the  $\text{Mn}^{3+}$  ions were placed in tetrahedral spinel sites. Table 1 shows the oxide formula, the corresponding cationic distribution and the  $\text{Mn}^{4+}/\text{Mn}^{3+}$  octahedral ratio obtained for each composition<sup>12</sup>.

Polarization curves for  $\text{O}_2$  reduction on the oxides were recorded between 298 and 338 K. Current values were corrected by diffusion effects and ohmic drop oxide/electrolyte, and oxygen solubility as a function of temperature was taken into consideration. The actual kinetic currents  $j_k$  were calculated using the equation  $j_k = j / (j_L - j)$ , where  $j$  and  $j_L$  are measured with limiting values.

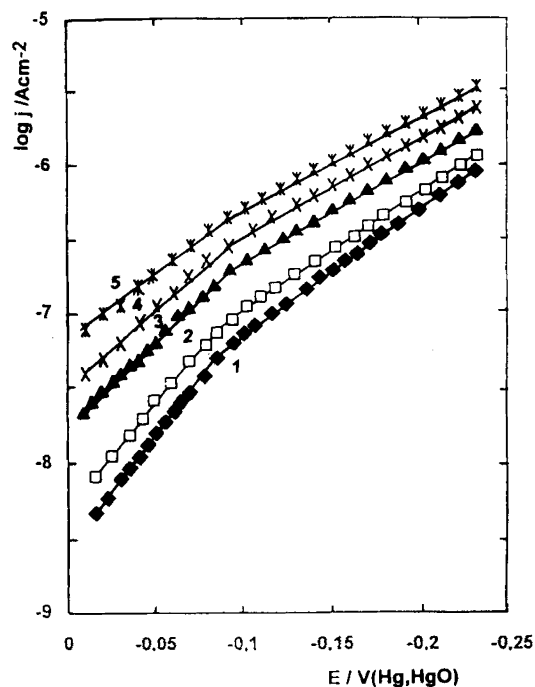
Figure 1 shows the lines  $E$ - $\log i$  obtained at five temperature values, using the most active oxide,  $\text{Cu}_{1.4}\text{Mn}_{1.6}\text{O}_4$ . Two Tafel slopes were observed. At l.p.  $(\partial E / \partial \log j) = -2.3$  RT/F, and at h.p. it was  $-2.3$  2RT/F. Tafel slope values increased with temperature, and they changed as follows:  $-65, -130$  (298 K);  $-70, -135$  (300 K);  $-75, -145$  (318 K);  $-80, -150$  (328 K) and  $-85, -155$  mV/dec (338 K) at l.p. and at h.p., respectively. The order with relation to oxygen is 1 in both regions. At low polarization, the  $\text{OH}^-$  order

changes from  $-1$  to  $-0.5$  for the oxide when  $x = 0.4$ . This order can decrease to  $-0.7$  when the copper concentration in the oxide decreases ( $x = 0$  and  $x = 0.1$ ). Current densities measured at a constant potential show a linear relationship with the inverse of temperature (Fig. 2). From the slope of these lines, we obtained the enthalpy of activation  $\Delta H^*$ . Defining the low region of potential as the zone between  $E = 0$  V and  $E = -0.08$  V and the high region being between  $E = -0.1$  V and  $E = -0.23$  V, it is possible to obtain from these lines, slopes on which  $\partial \log j / \partial (1/T) = -\Delta H^*_{l.p.} / R$  and  $\partial \log j / \partial (1/T) = -\Delta H^*_{h.p.} / R$ , according to Sepa *et al.*<sup>13</sup>. At any constant potential, the apparent enthalpy of activation increases when the pH increases. This is shown in Fig. 3 for a number of measurements in solutions with pHs ranging from 12 to 14.  $\Delta H^*_{E=0}$  was found to be 52 kJ/mole at  $\text{pH} = 12$  and 64 kJ/mole at  $\text{pH} = 14$ . In the lower current density region,  $\Delta H^*$  values were more sensitive to changes in the pH of the solution. The Tafel slopes of ORR on  $\text{Cu}_{1.4}\text{Mn}_{1.6}\text{O}_4$  decreased in a linear fashion when the temperature decreased in both potential regions (Fig. 4). From this linear relationship  $1/b$  vs.  $1/T$ , the following values of enthalpic and entropic components of transfer coefficients were obtained:  $\alpha_H = 1.8$  and  $\alpha_s = 3 \cdot 10^{-3} \text{ K}^{-1}$ . These values agree with the observed  $\Delta H$  -  $E$  dependence.

Similar curve shapes have been obtained with the other oxide compositions. In effect, it was found that  $\Delta H^*$  decreased with the substitution of manganese with copper in the structure from  $98 \pm 2$  kJ/mole to  $64 \pm 2$  kJ/mole (Table 1). This effect can be related to the manganese cation



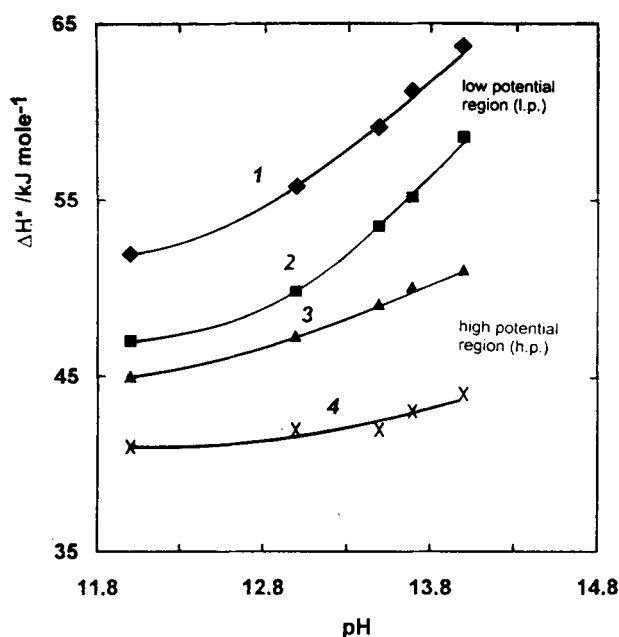
**Figure 1.** ORR Tafel slopes on the  $\text{Cu}_{1.4}\text{Mn}_{1.6}\text{O}_4$  electrode as a function of temperature (1) 298; (2) 308; (3) 318; (4) 328; (5) 338 K. Electrolyte 1 M KOH.



**Figure 2.**  $\log j - T^{-1}$  plot at a constant applied potential for ORR. Oxide:  $\text{Cu}_{1.4}\text{Mn}_{1.6}\text{O}_4$ . 1 M KOH. (1) 0; (2) 30; (3) 50; (4) 70; (5) 140; (6) 170; (7) 220 mV/ (Hg,HgO).

**Table 1.** Cationic distribution of the  $\text{Cu}_{1-x}\text{Mn}_{2-x}\text{O}_4$  oxide system and ORR apparent enthalpy of activation as a function of the  $\text{Mn}^{4+}/\text{Mn}^{3+}$  ratio.

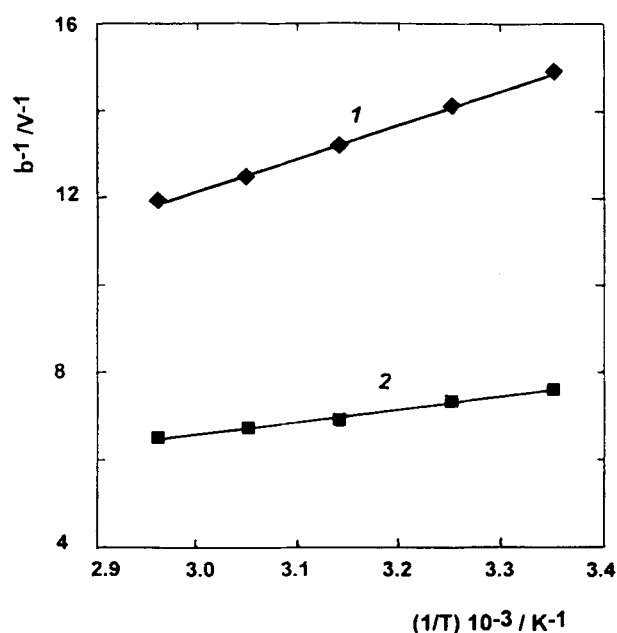
Oxide	Cationic distribution	$(\text{Mn}^{4+}/\text{Mn}^{3+})$	$\Delta H^*/\text{kJ mole}^{-1}$
$\text{CuMn}_2\text{O}_4$	$\text{Cu}^{+0.52}\text{Mn}^{2+0.48}[\text{Cu}^{2+0.48}\text{Mn}^{3+0.52}\text{Mn}^{4+}]$	1.9	$98 \pm 2$
$\text{Cu}_{1.1}\text{Mn}_{1.9}\text{O}_4$	$\text{Cu}^{+0.58}\text{Mn}^{2+0.42}[\text{Cu}^{2+0.52}\text{Mn}^{3+0.38}\text{Mn}^{4+1.1}]$	2.9	$89 \pm 2$
$\text{Cu}_{1.2}\text{Mn}_{1.8}\text{O}_4$	$\text{Cu}^{+0.59}\text{Mn}^{2+0.41}[\text{Cu}^{2+0.61}\text{Mn}^{3+0.19}\text{Mn}^{4+1.2}]$	6.3	$83 \pm 2$
$\text{Cu}_{1.3}\text{Mn}_{1.7}\text{O}_4$	$\text{Cu}^{+0.67}\text{Mn}^{2+0.33}[\text{Cu}^{2+0.63}\text{Mn}^{3+0.07}\text{Mn}^{4+1.3}]$	18.6	$72 \pm 2$
$\text{Cu}_{1.4}\text{Mn}_{1.6}\text{O}_4$	$\text{Cu}^{+0.70}\text{Mn}^{2+0.20}\text{Mn}^{3+0.10}[\text{Cu}^{2+0.70}\text{Mn}^{4+1.4}]$	—	$64 \pm 2$

**Figure 3.** Apparent enthalpy of activation - pH relationship for ORR at several applied potentials: (1) 0; (2) -30; (3) -70; (4) -140 mV/(Hg,HgO).

concentration placed in B sites of the spinel structure, in particular with the  $\text{Mn}^{4+}/\text{Mn}^{3+}$  ratio. This ratio decreases with  $x$  as  $\Delta H^*$  decreased monotonously with  $x$  (Fig. 5).

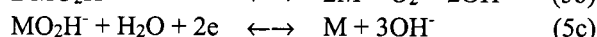
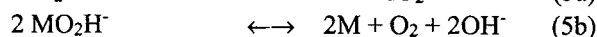
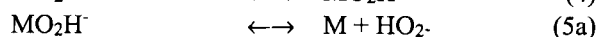
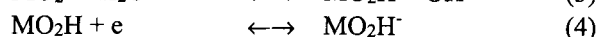
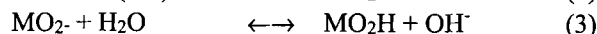
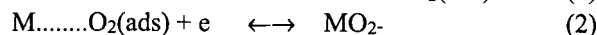
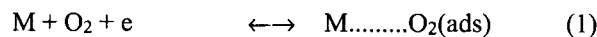
## Discussion

As has been shown, the Tafel slopes decrease when the temperature increases, making the ORR on copper manganite spinels more favorable at high temperature. Similar Tafel dependence has been observed in passivated iron<sup>17</sup> and platinum<sup>13</sup>. Considering the  $\Delta H^*$  values obtained as a function of applied potential, this makes physical sense if the components  $\alpha_H$  and  $\alpha_S$  are distinct from zero. In effect, for the oxide with  $x = 0.4$  these values are  $> 0$ . If the entropic and enthalpic factors also depend on the pH of the solution, then the  $\text{OH}^-$  order,  $\text{pOH}^-$ , increases (or decreases negatively) when the temperature decreases (Fig. 6). This phenomena can be related to a different way of adsorption species where the temperature changes. The effect of applied potential on  $\Delta H^*$  is shown in Fig. 2. At  $\text{pH} = \text{cst}$ , the enthalpy of activation at h.p.,  $\Delta H^*_{\text{h.p.}}$ , is higher than that at low potential  $\Delta H^*_{\text{l.p.}}$ . For instance, the oxide with  $x = 0.4$

**Figure 4.** Plots against  $1/T$  of Tafel slopes (1)  $b_1$ , and (2)  $b_2$  for the ORR at  $\text{Cu}_{1.4}\text{Mn}_{1.6}\text{O}_4$  electrodes.

has been determined at constant potential,  $\Delta H^*_{\text{h.p.}} = 44$  kJ/mole and  $\Delta H^*_{\text{l.p.}} = 64$  kJ/mole, showing that for all cases  $\Delta H^*_{\text{l.p.}} > \Delta H^*_{\text{h.p.}}$ . The different  $\Delta H^*$  values and Tafel slope values indicate that the ORR mechanism changes as a function of the applied potential.

The kinetic parameters of ORR obtained in this work, as well as the smooth transition of the kinetics, from that at low current characterized by  $\partial E/\partial \ln j = -RT/F$  to that at high current characterized by  $\partial E/\partial \ln j = -2RT/F$ , can be interpreted through the following mechanism similar to that proposed using copper manganites prepared by the ceramic method<sup>6</sup>:



Steps 5a, 5b and 5c can occur in parallel in different extensions, depending on the chemical nature and adsorp-

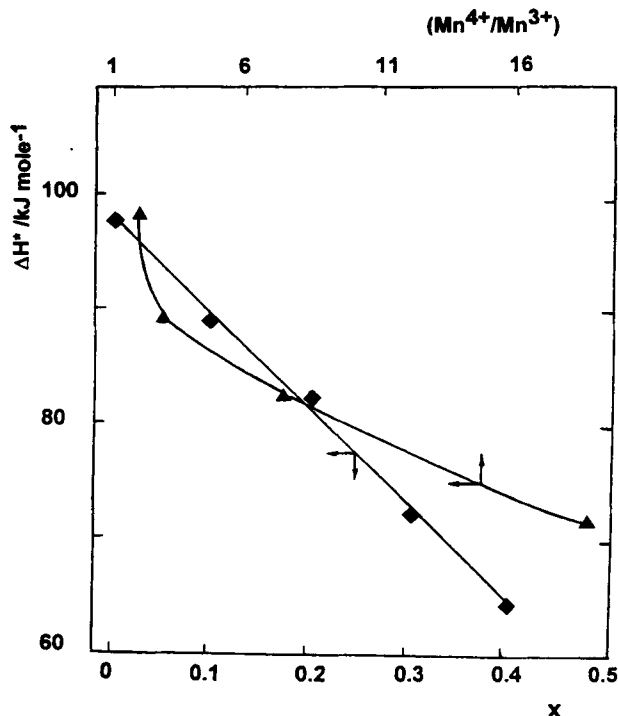


Figure 5. Apparent enthalpy of activation vs. oxide copper content ( $x$ ) and the  $[Mn^{4+}/Mn^{3+}]$  ratio relationship.

tion energy condition of the metal sites  $M$ . According to the original analysis<sup>6</sup>, the first step in the overall reaction pathway is the Pauling type adsorption of  $O_2$ , on a metallic surface site. In this mechanism, at  $pH = 14$  and using the oxide with  $x = 0.4$  at 298 K, the rate determining step is the Reaction 3, occurring in the high potential region. At low potential, with a low Tafel slope, the second electron transfer is the rds (4).

The fractional reaction order with respect to  $OH^-$  of  $-1/2$  observed at h.p. with the oxides prepared by the spray pyrolysis studied in this work, cannot be interpreted in terms of any simple electrode kinetic conception, e.g., with Langmuirian adsorption conditions as in the preceding case. In this case, we thought that the first step would be the rds, if we assume (i) that the adsorption of  $HO_2^-$  is of the Temkin type, thus implying  $0.2 \leq \theta_{HO_2^-} \leq 0.8$ , where  $\theta_{HO_2^-}$  is the coverage of the surface in  $HO_2^-$  groups, and (ii)  $\theta \approx \theta_T$ , where  $\theta_T$  is the total coverage by all adsorbed species ( $O_2$ ,  $O_2^-$ ,  $HO_2$ ,  $HO_2^-$ ,  $OH^-$ ). It is well known that the Temkin isotherm can be written:

$$r \theta / RT = \ln C_{OH^-} + FE / RT + \text{cst.} \quad (1)$$

The current expression for the rds is:

$$i = n F k_1 p_{O_2} \exp \{-\alpha \Delta G_{\text{ads}} / RT\} \quad (2)$$

where  $\alpha$  is the symmetry factor associated with standard Gibbs energy,  $\Delta G_{\text{ads}}$ , which is related to surface coverage,  $\theta$ :

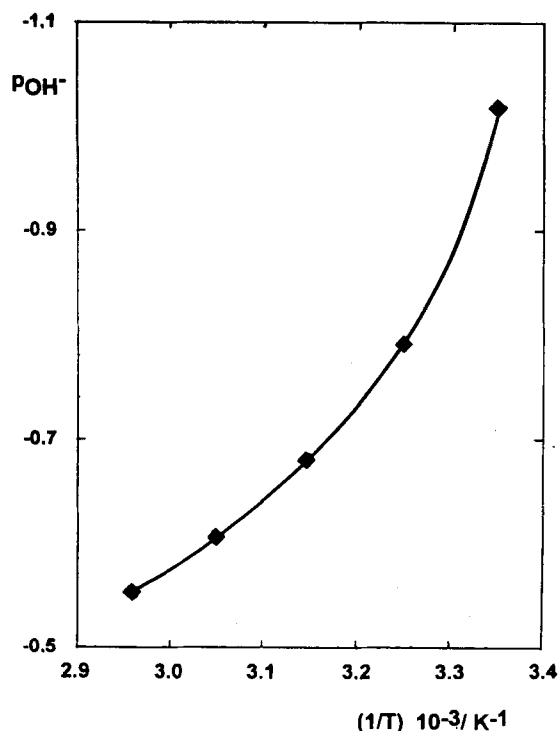


Figure 6. The temperature dependence on reaction order  $p_{OH^-}$  at  $-0.07 V$  using a  $Cu_{1.4}Mn_{1.6}O_4$  electrode.

$$\Delta G_{\text{ads}} = \Delta G_{\text{ads}}^0 + r\theta \quad (3)$$

and  $r$  is the adsorbed molecule interaction parameter, and  $\Delta G_{\text{ads}}^0$  is the Gibbs energy when  $\theta < \theta_T$ . Assuming that  $\Delta G$  is related to  $\theta$  by Eq. 14:

$$\Delta G_{\text{ads}}^0 / RT = \Delta G_{\text{ads}}^0 / RT + \alpha r \theta / RT \quad (4)$$

using the following constant parameter:  $k_0 = \exp \{-\alpha r \theta / RT\}$ , it is possible to obtain the above expression in an exponential form:

$$\exp \{-\beta \Delta G_{\text{ads}} / RT\} = k_0 \exp \{-\alpha r \theta / RT\} \quad (5)$$

From Eqs. 1, 2 and 5 with  $K = k_1 k_0 = \text{cst}$ , the following expression of current density is derived:

$$i = n F K p_{O_2} C_{OH^-}^{-\alpha} \exp \{-\alpha FE / RT\} \quad (6)$$

In a typical case where  $\alpha = 0.5$ , the order of the reaction at  $E = \text{constant}$  with respect to the oxygen is  $(d \log j / d \log p_{O_2})_{C_{OH^-}, E} = 1$ , and with respect to the  $OH^-$  concentration it is  $(d \log j / d \log C_{OH^-})_{E, p_{O_2}} = -0.5$ , and the Tafel slope is  $(dE / d \log j)_{C_{OH^-}, p_{O_2}} = -120 \text{ mV dec}^{-1}$ . Our data fit this model.

It is clear that the two Tafel regions observed in this work are related through different adsorption modes occurring on the electrocatalytic metal surface sites  $M$ , and therefore different  $\Delta H^*$  values are attained.

The active adsorption sites M in our series of oxides will be  $Mn^{3+}$  and  $Mn^{4+}$  because the bond strength of cations with a high degree of oxidation is stronger than those with low oxidation. Considering that the  $Mn^{4+}$  concentration increases with x, and that  $\Delta H^*$  decreases in the same way, the active sites of adsorption may be  $Mn^{4+}$  rather than  $Mn^{3+}$ .

## Conclusion

The present study shows that the enthalpy of activation in a low potential region (with a Tafel slope of 60 mV/dec) is different from the enthalpy of activation in a high potential region (with a Tafel slope of 120 mV/dec). This change can indicate that something is changing in the ORR mechanism, such as the rds in the function of degree of polarization. The different Tafel slopes can be the consequence of a change in the adsorption conditions of the intermediate oxygen species with the coverage  $\theta$ . The ORR is pH and temperature dependent according to the determined activation enthalpy values. The enthalpy changes with the oxide composition and with the surface site concentrations showing that the oxygen reduction not only depends on electrolyte properties but on the  $Mn^{4+}/Mn^{3+}$  ratio, where the  $Mn^{4+}$  ions are the most important sites.

## Acknowledgments

Financial support from the Consejo Nacional de Investigaciones Científicas y Técnicas (CONICYT-Santiago, grant Fondecyt 123/92), the Univ. de Antofagasta, and the Univ. de Santiago (DICYT) are gratefully acknowledged.

## References

1. E.J.M. O'Sullivan and E.J. Calvo *Electrode Kinetics: Reactions* (R.G. Compton, Ed., Elsevier, Amsterdam, 1987), p. 247.
2. J.L. Gautier *Electrocatalisis Temáticas Especiales* (A.J. Arvia and C.M. Marschoff, Eds., FECIC, Buenos Aires, 1983), p. 442.
3. J. Brenet, *27th Meet. ISE*, Zurich, Sept. 1976.
4. H. Nguyen Cong, P. Chartier and J. Brenet, *J. Appl. Electrochem.* **7**, 383 (1977).
5. A. Restovic, J.L. Gautier, G. Poillerat and P. Chartier, *43th Meet. ISE*, Córdoba, Sept. 1992.
6. J.L. Gautier, A. Restovic and P. Chartier, *Bol. Soc. Chil. Quim.* **33**, 209 (1988).
7. J.L. Gautier, A. Restovic and P. Chartier, *J. Appl. Electrochem.* **19**, 28 (1989).
8. M.R. Tarasevich and B.N. Efremov *Electrodes of Conductive Metallic Oxides, Part A* (S. Trasatti, ed., Elsevier, Amsterdam, 1980), p. 221.
9. A. Restovic, G. Poillerat, J.F. Koenig, P. Chartier and J.L. Gautier, *Thin Solid Films* **199**, 139 (1991).
10. B.E. Conway *Modern Aspects of Electrochemistry* (B.E. Conway, R.E. White and J. O'Bockris, eds., Plenum Press, N.Y., 1985).
11. D.B. Sepa, M.V. Vojnovic, Lj.M. Vracar and A. Damjanovic, *Electrochim. Acta* **31**, 91 (1986).
12. A. Restovic, *Thesis*, Strasbourg, 1992.
13. D.B. Sepa, M.V. Vojnovic, Lj. M. Vracar and A. Damjanovic, *Ibid* **31**, 97 (1986).
14. L. Bahadur, M. Hamdani, J.F. Koenig and P. Chartier, *Solar Energy Materials* **14**, 107 (1986).
15. R.E. Vandenberghe, G.G. Robbrecht and V.A.M. Brabers, *Mat. Res. Bull.* **8**, 571 (1973).
16. J. Brenet and P. Faber, *J. Power Sources* **4**, 203 (1979).
17. V. Jovancicevic and J. O'Bockris, *J. Electrochem. Soc.* **133**, 1797 (1986).